






Deletion of SUMO1 attenuates behavioral and anatomical deficits by regulating autophagic activities in Huntington disease

Uri Nimrod Ramírez-Jarquín^a, Manish Sharma^a, Wuyue Zhou^a , Neelam Shahani^{a,1} , and Srinivasa Subramaniam^{a,1} 

^aDepartment of Neuroscience, The Scripps Research Institute, Jupiter, FL 33458

Edited by Christopher Ross, Department of Psychiatry, Johns Hopkins University, Baltimore, MD; received April 18, 2021; accepted December 13, 2021, by Editorial Board Member Jeremy Nathans

The CAG expansion of huntingtin (mHTT) associated with Huntington disease (HD) is a ubiquitously expressed gene, yet it prominently damages the striatum and cortex, followed by widespread peripheral defects as the disease progresses. However, the underlying mechanisms of neuronal vulnerability are unclear. Previous studies have shown that SUMO1 (small ubiquitin-like modifier-1) modification of mHTT promotes cellular toxicity, but the *in vivo* role and functions of SUMO1 in HD pathogenesis are unclear. Here, we report that SUMO1 deletion in Q175DN HD-het knockin mice (HD mice) prevented age-dependent HD-like motor and neurological impairments and suppressed the striatal atrophy and inflammatory response. SUMO1 deletion caused a drastic reduction in soluble mHTT levels and nuclear and extracellular mHTT inclusions while increasing cytoplasmic mHTT inclusions in the striatum of HD mice. SUMO1 deletion promoted autophagic activity, characterized by augmented interactions between mHTT inclusions and a lysosomal marker (LAMP1), increased LC3B- and LAMP1 interaction, and decreased interaction of sequestosome-1 (p62) and LAMP1 in DARPP-32-positive medium spiny neurons in HD mice. Depletion of SUMO1 in an HD cell model also diminished the mHTT levels and enhanced autophagy flux. In addition, the SUMOylation inhibitor ginkgolic acid strongly enhanced autophagy and diminished mHTT levels in human HD fibroblasts. These results indicate that SUMO is a critical therapeutic target in HD and that blocking SUMO may ameliorate HD pathogenesis by regulating autophagy activities.

striatal vulnerability | posttranslational modification | gene expression | motor abnormality | neurodegeneration

Expansion mutation of the CAG repeat in the huntingtin (HTT) gene causes the motor disturbance, cognitive loss, and psychiatric manifestations associated with Huntington disease (HD). HD results in the degeneration of the striatum with subsequent loss of corticostriatal white-matter connections (1). The mutant HTT (mHTT) affects multiple signaling and pathways; however, the underlying pathogenic mechanism that causes the HD is unknown (2). The mHTT protein is controlled in a cell/tissue/region-specific manner (3–5), but it is unclear how it may contribute to HD neuronal vulnerability.

Multiple lines of evidence point to an aberration in autophagy—an essential degradative pathway that maintains neuronal homeostasis—as the major feature of neurodegeneration (6). Studies have implicated aberrant autophagy in HD, as well as a failure of autophagic processes such as cargo loading, in the accumulation of mHTT and the progression of the disease (7–9). Normal HTT serves as an autophagy scaffold and interacts with the Atg8 homologs ULK1 and p62 during autophagy, but the molecular mechanism and the precise role of mHTT in autophagy dysregulation remain elusive (10–12). Accordingly, molecular and pharmacological agents that can promote autophagy are being actively tested in preclinical models (13–18). Nevertheless, the actual alterations in autophagy homeostasis and the treatments

that can lead to its restoration are unknown (12). This gap in knowledge remains a major hurdle in identifying targets for successful treatment of HD.

One potential target is the small ubiquitin-like modifier (SUMO), which consists of three ubiquitously expressed paralogs in vertebrates: SUMO1, SUMO2, and SUMO3. It is a conserved ~10.5-kDa protein modifier that attaches covalently to lysine residues on multiple substrate proteins in a dynamic and reversible manner in a process known as SUMOylation. Protein modification by SUMO is implicated in a diverse array of neurological disorders and is known to regulate a wide range of cellular processes, including gene expression, nuclear transport, signal transduction, and apoptosis, but its mechanistic connection to neurodegenerative disease is less clear.

We have reported that a striatal enriched protein, Rhes, is SUMO modified on multiple lysine residues and serves as a physiological regulator of SUMOylation and gene transcription (19, 20). The mHTT is modified by SUMO1, and Rhes further enhances SUMO1 modification (21–23). SUMO1 modification of mHTT increases the solubility of mHTT, promotes cellular toxicity (23), and enhances Rhes-mediated transport of vesicle-bound mHTT via tunneling-like nanotubes (24). Accordingly, Rhes deletion ameliorates, and Rhes overexpression worsens,

Significance

SUMO protein can decorate other proteins via a process called SUMOylation that can regulate toxicity of proteins linked to neurodegenerative diseases. The mutant huntingtin (mHTT) protein in Huntington disease (HD) degenerates nerve cells, and SUMOylation of mHTT makes it more soluble and more toxic to the nerve cells. Here, we show that SUMO deletion in a humanized mouse HD model depletes mHTT and prevents brain shrinkage and behavioral abnormalities. SUMO deletion blocked inflammation and enhanced autophagy, a beneficial cellular degradation pathway. Importantly, ginkgolic acid (GA), a widely used plant supplement that can inhibit SUMOylation, activates autophagy and promotes the degradation of mHTT in human HD cells. Thus, our study indicates GA and analogs might be therapeutically beneficial to HD patients.

Author contributions: U.N.R.-J., M.S., N.S., and S.S. designed research; U.N.R.-J., M.S., W.Z., N.S., and S.S. performed research; U.N.R.-J., M.S., W.Z., N.S., and S.S. analyzed data; and N.S. and S.S. wrote the paper.

The authors declare no competing interest.

This article is a PNAS Direct Submission. C.R. is a guest editor invited by the Editorial Board.

This article is distributed under [Creative Commons Attribution-NonCommercial-NoDerivatives License 4.0 \(CC BY-NC-ND\)](https://creativecommons.org/licenses/by-nc-nd/4.0/).

¹To whom correspondence may be addressed. Email: nshahani@scripps.edu or ssubrama@scripps.edu.

This article contains supporting information online at <http://www.pnas.org/lookup/suppl/doi:10.1073/pnas.2107187119/-DCSupplemental>.

Published January 27, 2022.

the HD phenotype in HD cell models (primary neurons, mouse cells, and human embryonic stem cell-derived medium spiny neurons [MSNs]) and HD mouse models (25, 26). Recently, Rhes has been linked to tau-mediated pathology involving SUMOylation, and Rhes alterations are now identified as a novel hallmark of tauopathies (27, 28). Thus, Rhes–SUMO signaling pathways participate in neurodegenerative disease processes by modulating disease-relevant proteins.

However, no mechanisms or systematic evaluations have been identified to explain how SUMO might determine the course of neuronal decline and eventual striatal atrophy in slowly progressing knockin HD mouse models. Here, we deleted SUMO1 in the Q175DN HD-het (Q175DN) knockin mouse model of HD (29), which contains the human HTT exon 1 with expanded CAG repeats, and we characterized the resulting Q175DN-SUMO1KO mouse line longitudinally to determine the role of SUMO1 in terms of the nature, extent, and age of onset of behavioral deficits. We also performed anatomical, molecular, and biochemical signaling in the striatal tissues. Finally, we evaluated the effect of SUMO1 deletion or pharmacological SUMO inhibition on biochemical signaling by using HD mouse and human cell-culture models.

Results

SUMO1 Deletion Diminishes HD-Associated Behavioral Deficits in Q175DN Mice. To determine the role of SUMO1 in HD pathogenesis using HD knockin mice (neomycin-deleted Q175DN HD-het [Q175DN] mice (29), we generated HD-het mice lacking a SUMO1 gene (Q175DN-SUMO1KO). We longitudinally subjected the wild-type (WT, $n = 37$ /mixed sex ratio), Q175DN ($n = 28$ /mixed sex ratio), Q175DN-SUMO1KO ($n = 30$ /mixed sex ratio), and SUMO1KO ($n = 27$ /mixed sex ratio) mice to repeated behavioral tests beginning at ~2 mo of age at 2-mo intervals until the mice reached ~12 mo of age (see scheme in Fig. 1A). Motor coordination and balance of mice were measured using an accelerating-rotarod and beam-walking tests. First, in the accelerating-rotarod test, Q175DN-het mice showed a significant progressive decrease in latency to fall (fell faster from the rotarod) beginning at 4 mo of age compared with the WT mice, consistent with previous reports (29, 30). In contrast, upon SUMO1 deletion in HD mice (Q175DN-SUMO1KO), the rotarod deficits were observed beginning at 10 mo of age compared with the WT mice (Fig. 1B). This result indicated that SUMO1 deletion in Q175DN-het mice delays the rotarod deficit by 6 mo, which is highly significant. Similarly, we found a progressive increase in beam-walk deficits (time to cross the beam) beginning at 4 mo of age in Q175DN mice compared with WT mice, and SUMO1 deletion in HD mice delayed these deficits by 6 mo (Fig. 1C). To measure general locomotor activity, mice were subjected to an open field test. A significant decrease in the total activity was observed in Q175DN mice beginning at 6 mo of age compared with WT mice that progressively decreased with age. However, in SUMO1-deleted HD mice, the open field deficits were observed only around 10 mo of age (Fig. 1D). We found that anxiety-like behaviors (the duration/frequency in the center/sides and corner) were highly variable in WT mice with age (SI Appendix, Fig. S1). Q175DN mice showed a subtle but significant decline in these behaviors with age (SI Appendix, Fig. S1). Q175DN-SUMO1KO showed some protection at 10 mo on selected behaviors (SI Appendix, Fig. S1). SUMO1KO also showed a transient deficit in the anxiety-like symptoms at 8 mo compared with WT (SI Appendix, Fig. S1). Altogether, these longitudinal behavioral analyses indicate that SUMO1 deletion diminished HD-like motor and some age-linked anxiety-like deficits in Q175DN mice.

A slight (~20%) decrease in body weight was noted at about 10 mo of age in the Q175DN mice when compared with WT,

consistent with previous reports (29, 31), but it was not significantly different in Q175DN-SUMO1KO mice (Fig. 1E). This indicates that SUMO1 does not modulate nonmotor metabolic dysfunction, such as body weight, in HD.

We also employed a battery of behavioral tests to quantify the neurological dysfunction. These tests include walking on a ledge, clapping, gait, kyphosis (spine curvature), and tremor, which can be averaged as a “composite” score (32). Behavioral battery tests revealed that Q175DN mice performed worst on ledge, clapping, gait, kyphosis, and tremor testing, but the performance on these tasks was significantly better in Q175DN-SUMO1KO mice in both individual tests and composite scores (Fig. 1F and G). We found around 60% protection in the behavioral battery test (composite score) in SUMO1-deleted HD mice compared with HD mice (Fig. 1G). Thus, SUMO1 deletion attenuated the extent and severity of motor and neurological abnormalities associated with HD.

We also determined whether SUMO1 had any effect on the sex differences in rotarod deficits. Compared with females, male Q175DN mice showed a consistent decline in age-dependent rotarod deficits (SI Appendix, Fig. S2A). SUMO1 deletion led to age-dependent protection on rotarod deficits in male Q175DN-SUMO1KO mice at all the age points, while in female groups, significant protection was observed only at 6 and 8 mo (SI Appendix, Fig. S2A). Both female and male Q175DN mice showed similar deficits on behavioral battery tests, which are diminished in both male and female Q175DN-SUMO1KO groups (SI Appendix, Fig. S2B). Thus, SUMO1-KO had no considerable sex differences in preventing the HD-like deficiencies in the Q175DN model.

SUMO1 Deletion Abolishes Striatal Atrophy in HD Mice. We next analyzed whether the behavioral protection induced by SUMO1 deletion is accompanied by changes in anatomical deficits. We determined brain atrophy by estimating the lateral ventricles’ area enlargement and volume measurement of the striatum and corpus callosum using stereology by the Cavalieri method. For this analysis, we used five mice/group (male = 3, female = 2), four different areas, and up to four brain sections with a description of the distance between the sections in Materials and Methods (SI Appendix). We observed lateral ventricle enlargement in the Q175DN mice in the frontal, central, and caudal striatum regions (Fig. 2A and B). These anatomical data results are consistent with those previously published studies in Q175DN mice (29, 33). Interestingly, SUMO1 deletion in HD mice (Q175DN-SUMO1KO) dramatically diminished the lateral ventricle enlargement in all three striatal regions (Fig. 2A and B). Striatal volume as well as corpus callosum volume were also diminished in Q175DN (Fig. 2C and D). The lateral ventricle size, striatal volume, and corpus callosum volume in Q175DN-SUMO1KO were comparable to those of the WT and SUMO1KO control groups (Fig. 2A–D). Thus, SUMO1 deletion almost completely prevented the striatal atrophy observed in the knockin HD mice.

Effect of SUMO1 Deletion on the Striatal Gene Expression Landscape in HD Mice. Transcriptional dysregulation is a major event in HD pathogenesis, and SUMO is involved in the transcriptional repression as well as activation functions. We therefore examined whether SUMO1 impacts motor deficits and striatal atrophy in HD (Figs. 1 and 2) by a dysregulation of gene expression. We performed a genome-wide striatal tissue-specific gene expression pattern analysis by comparing RNA sequencing (RNA seq) in the striatum of 13-mo-old WT, Q175DN, Q175DN-SUMO1KO, and SUMO1KO mice (one male and one female mice striata were pooled/experiment, $n = 3$ experiment/genotype, total = 6 mice/genotype, total = 24 mice). Gene counts revealed 1,042 genes that were significantly up-regulated

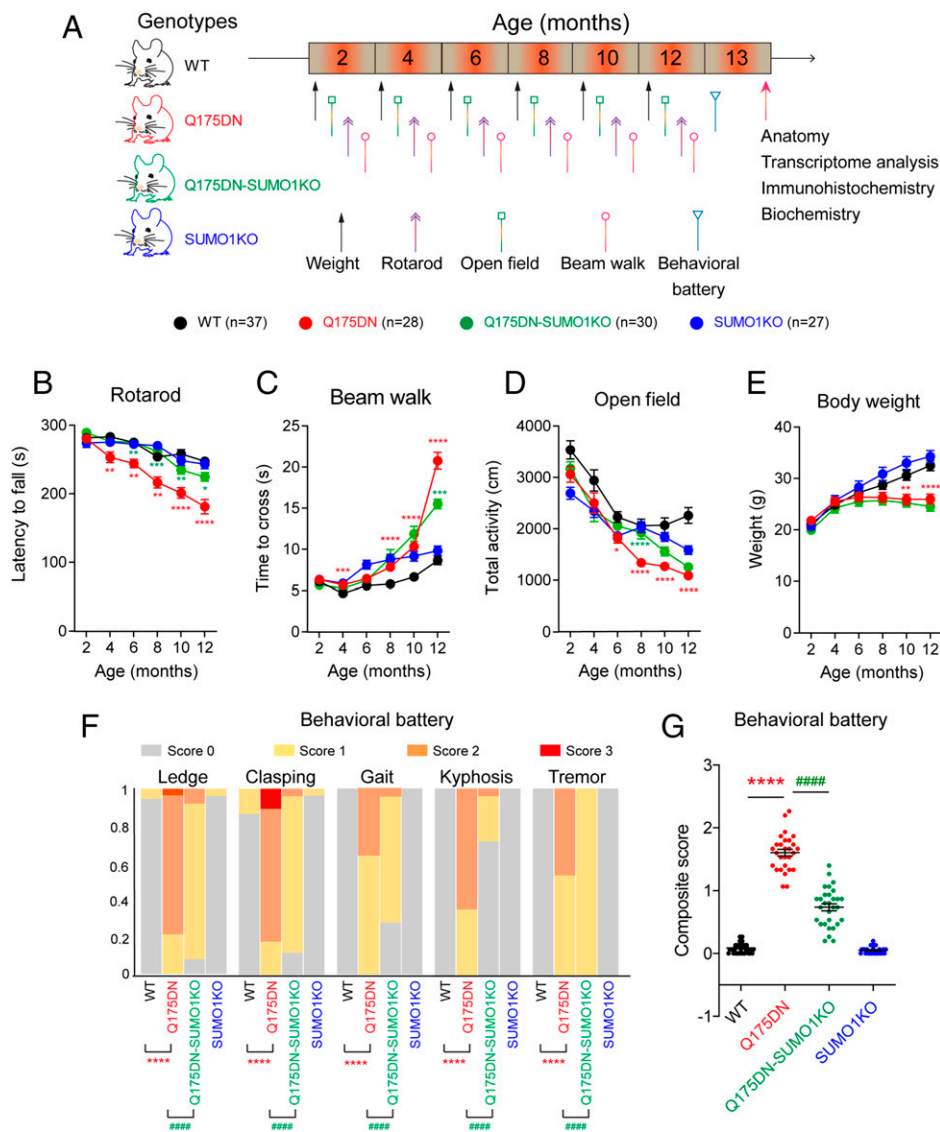


Fig. 1. Effect of SUMO1 deletion on age-associated motor abnormalities in the Q175DN knockin HD mice model. (A) Shows the genotypes, time line, and experimental design for the animal study. (B–G) Behavioral and body-weight analysis at 2 to 12 mo of age; rotarod (B), beam walk (C), open field (D), body weight (E) and behavioral battery (F), and behavioral battery composite score (G). Behavioral batteries included the ledge test, clasp, gait, kyphosis, and tremor evaluation. The frequency of each behavior according to the genotype is shown in F; a composite score for all the behavioral battery is shown in G. Data are mean \pm SEM (WT [male = 22, female = 15], Q175DN [male = 19, female = 9], Q175DN-SUMO1KO [male = 13, female = 17], and SUMO1KO [male = 15, female = 12]). * P < 0.05, ** P < 0.01, *** P < 0.001, and **** P < 0.0001 by two-way ANOVA mixed-effects model followed by Tukey's multiple comparison test (for B–E). In B–E, a green asterisk is between Q175DN-SUMO1KO versus Q175DN. A red asterisk is between Q175DN versus WT. **** P < 0.0001 between Q175DN and WT; **** P < 0.0001 between Q175DN-SUMO1KO and Q175DN by Fisher's exact test (for F), and **** P < 0.0001 between Q175DN and WT; **** P < 0.0001 between Q175DN-SUMO1KO and Q175DN by one-way ANOVA followed by Tukey's multiple comparison test (for G).

and down-regulated (p -value adjusted, $\text{padj} < 0.05$) in the Q175DN HD-het mice compared with the WT striatum (Dataset S1). Ingenuity pathway network analysis (IPA) revealed significant alterations in canonical pathways, such as cAMP-response element binding protein (CREB), opioid signaling, endocannabinoid signaling, G protein-coupled receptors (GPCR), and glutamate receptor signaling, as well as fragile X mental retardation 1 (FMR1) signaling, between the WT and Q175DN striatum (SI Appendix, S3 A and B and Dataset S1). Some of these altered pathways in Q175DN have been previously reported (34). However, we found very few differentially expressed genes between Q175DN-SUMO1KO and Q175DN mice striatum ($\text{padj} < 0.05$). Of the 18 genes differentially expressed, 13 were up-regulated and 5 were down-regulated (SI Appendix, Fig. S3C). Loss of SUMO1 in HD mice leads to up-regulation of selected genes such as aldehyde oxidase 4, an enzyme that oxidizes aldehyde implicated in circadian rhythm and locomotor activities was up-regulated (35). Also, SUMO1 deletion in HD mice leads to the down-regulation of genes, such as SP110 nuclear body proteins, that act as transcriptional coactivators (36) in the HD striatum (SI Appendix, Fig. S3C). Multiple genes with unknown functions are also altered by SUMO1 deletion. Due to the small number of gene alterations, IPA analysis

did not identify a comprehensive network of biological processes or pathways, as the number of connectible entities with sufficiently high z-scores was insufficient. However, IPA did hint that the modulated genes belonged to hypoxia, circadian rhythm, DNA methylation, and inflammatory processes (SI Appendix, Fig. S3D) in Q175DN-SUMO1KO compared with Q175DN mice striatum. We found significant alterations of 255 genes between WT and SUMO1KO mice ($\text{padj} < 0.05$) and of 2308 genes between SUMO1KO and Q175DN mice ($\text{padj} < 0.05$); most of the altered genes involved opioid signaling, CREB signaling, and GPCR signaling, among others (Dataset S1 and SI Appendix, Fig. S3 E and F). These results indicate that SUMO1 has only a nominal impact on the overall gene expression changes occurring in the HD striatum, suggesting that SUMO1 may promote HD-related motor deficits and striatal atrophy via posttranscriptional and/or posttranslational mechanisms.

SUMO1 Deletion Prevents the Inflammatory Responses of HD. Since the IPA analysis suggested that the linked altered genes were functionally enriched in inflammatory responses in Q175DN-SUMO1KO compared with Q175DN mice striatum (SI Appendix, Fig. S3D), we carried out glial fibrillary acidic protein (GFAP) immunoreactivity assays to assess the inflammatory

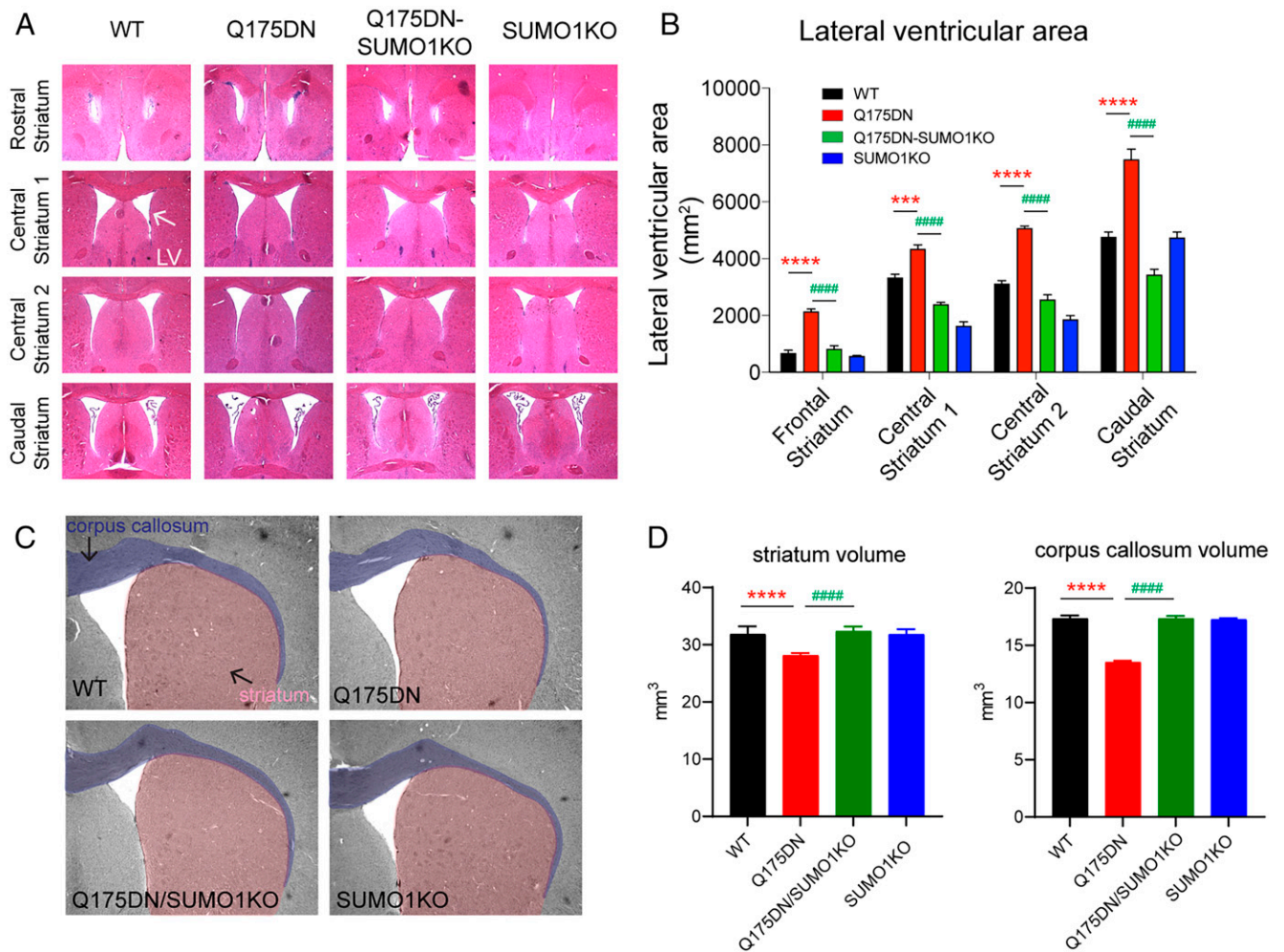


Fig. 2. Effect of SUMO1 deletion on striatal anatomical changes in Q175DN mice. (A) Representative H&E-stained sections for rostral (+1.45 from bregma), central striatum 1 (+1.0 from bregma), central striatum 2 (+0.60 from bregma), and caudal (+0.1 from bregma) lateral ventricles (LV, arrow) at the striatum level from the indicated genotypes. (B) Quantification of the lateral ventricular area from A. (C and D) Histological sections and quantification to illustrate the corpus callosum, striatum, and ventricular changes in all the genotypes: corpus callosum (purple) and striatum (pink). For B and D, data are mean \pm SEM ($n = 5$ mice per group [male = 3, female = 2]). Three to four sections were analyzed and averaged for each striatal region per mouse. **** $P < 0.001$, **** $P < 0.0001$, ##### $P < 0.0001$, two-way ANOVA followed by Tukey's multiple comparison test.

changes within the frontal, central, and caudal regions of striatal sections from the WT, Q175DN, Q175DN-SUMO1KO, and SUMO1KO mice (Fig. 3A). GFAP expression was strikingly enhanced in all regions, with a slightly increased signal in the central striatum in Q175DN mice compared with WT mice (Fig. 3A and B). The Q175DN-SUMO1KO mice showed a marked decrease in GFAP immunoreactivity in all three striatal regions compared with the Q175DN mice (Fig. 3A, c and e and B). GFAP immunoreactivity was unaltered between the WT and SUMO1KO striatum (Fig. 3A and B). Higher GFAP expression is also seen in the cortical region of Q175DN mice (Fig. 3A, d), which is also diminished in the Q175DN-SUMO1KO (Fig. 3A, f).

Western blot analysis of the striatal tissue further confirmed that GFAP protein expression, but not messenger RNA (mRNA) expression, was significantly reduced in the Q175DN-SUMO1KO mice compared with the Q175DN mice (SI Appendix, Fig. S4 A–C). The protein levels of DARPP-32, a commonly used biochemical MSN marker for striatal damage in HD, was diminished in Q175DN mice compared with WT mice (SI Appendix, Fig. S4 A and B). This reduction is likely due to diminished DARPP-32 mRNA in Q175DN mice (SI Appendix, Fig. S4C). The Q175DN-SUMO1KO mice showed a similar extent of loss of DARPP-32 protein and mRNA, indicating SUMO1 may not interfere with

the transcriptional down-regulation of DARPP-32 in the HD striatum (SI Appendix, Fig. S4C). Interestingly, not all striatal genes are down-regulated in the striatum of Q175DN compared with WT. While *Darpp-32*, *Drd1a*, *Drd2*, and *pde10a* are down-regulated, *Adora 1*, *Foxp1*, *Rasgrp2* or *St8sia3*, and *Gng7* remain unaffected (Dataset S1). Thus, mHtt may alter only the subset of mRNA expressions in the striatum without affecting the striatal cell numbers in the Q175DN mice independent of SUMO1. Interestingly, we also found activation of inflammatory marker microglia as evidenced by Iba1 up-regulation in Q175DN striatum. SUMO1 deletion completely prevented Iba1 protein and mRNA up-regulation in Q175DN-SUMO1KO (SI Appendix, Fig. S4 D and E). Together, these results indicate that SUMO1 deletion prevents the striatal atrophy that is accompanied by a strong reduction in the inflammatory responses in the striatum. Therefore, SUMO1 deletion may prevent the striatal atrophy by alterations in the corpus callosum, shrinkage of neuronal arborization, and corticostriatal network dysfunction as well as diminished inflammatory responses.

SUMO1 Deletion Enhances EM48+ Aggregates and Decreases Soluble Forms of HTT. As SUMO plays a major role in regulating protein aggregation, including aggregation of mHTT (22, 23), we first

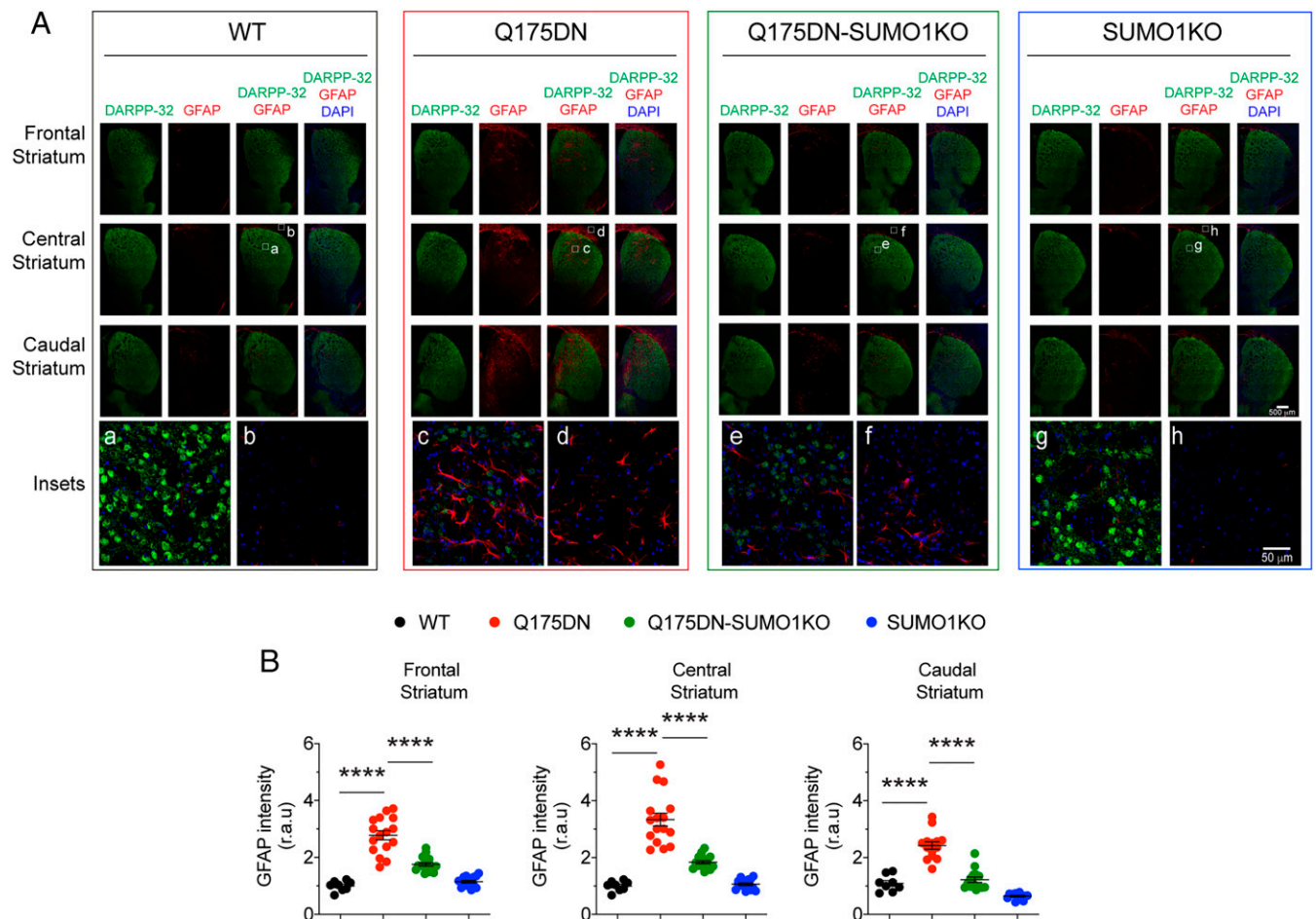


Fig. 3. SUMO1 deletion diminishes inflammatory astroglial response in Q175DN mice. (A) Representative confocal images for the frontal, central, and caudal striatum showing DARPP-32 (green), GFAP (red) IHC, and nuclear stain DAPI (blue) with the magnified image in the insets from the indicated genotypes. Striatum (a, c, e, and g) and cortex (b, d, f, and h). (B) Quantification of the GFAP intensity from the frontal, central, and caudal striatum. Data are mean \pm SEM, $n = 5$ mice per group (male = 3; female = 2); between one and three sections for each striatal region per mouse were analyzed (in total, eight sections for WT and 16 sections each for Q175DN, Q175DN-SUMO1KO, and SUMO1KO groups). **** $P < 0.0001$ by one-way ANOVA followed by Tukey's multiple comparison test.

analyzed the aggregated and soluble forms of mHTT by Western blotting. We used EM48 antibody, the most sensitive antibody for detecting mHTT inclusions, as well as MAB2166 (amino acids 442 through 457), polyQ (clone 3B5H10), and HTT (D7F7) antibodies to detect full-length (FL) Htt.

Western blotting analysis of striatal brain lysates prepared in nondenaturing Tris buffer [which enriches cytoplasmic proteins (37, 38)] showed a significant enhancement of EM48+ Htt aggregates in the Q175DN-SUMO1KO striatum compared with the Q175DN striatum (Fig. 4A and B). As expected, the EM48+ Htt aggregates were not seen in WT and SUMO1KO control groups (Fig. 4A). We then probed the same lysates for MAB2166 antibody (which detects both Htt and mHTT) or polyQ antibody to detect mHTT. We found diminished levels of Htt protein in the Q175DN mice striatum, consistent with earlier reports (39, 40), but a further diminishment of Htt and decrease in polyQ mHTT in the Q175DN-SUMO1KO striatum (Fig. 4A, C, and D). Note that normal Htt protein levels are also diminished in SUMO1KO striatum (Fig. 4A and C). Next, we determined if SUMO1 regulates the *HTT* mRNA. We found that while *HTT* mRNA is significantly diminished in the Q175DN mice compared with WT, it remained diminished to a similar extent in the Q175DN-SUMO1KO mice. The mRNA of normal *HTT* is similar between WT and SUMO1KO striatum (Fig. 4E). Investigation with HTT D757 (antibody epitope

around proline1220) revealed diminished Htt levels upon SUMO1 deletion (SI Appendix, Fig. S5). Thus, SUMO1 deletion reduces the protein levels of mHTT as well as normal Htt, but not their mRNA levels, in the striatum, indicating posttranscriptional and/or posttranslational mechanisms.

Although western blotting data showed that SUMO1 deletion diminishes the soluble mHTT but increases the aggregated forms of mHTT (EM48+), the whole tissue Western cannot distinguish the cellular localization of mHTT. Therefore, we carried out immunohistochemistry (IHC) to determine the EM48 distribution. IHC staining of striatal brain sections of WT or SUMO1KO mice with EM48 antibody did not reveal any Htt inclusions, so these mice were not included in further analysis. However, EM48 antibody readily detected Htt aggregates in Q175DN and Q175DN-SUMO1KO striatal brain sections in both the cortex and striatum (Fig. 4F), consistent with previous reports (29). The numbers of DARPP-32+ neurons between Q175DN and Q175DN-SUMO1KO mice did not differ (Fig. 4G and H); however, a stronger colocalization of EM48+ punctate was observed in DARPP-32+ MSNs (Fig. 4G and I) in the striatum of Q175DN-SUMO1KO mice than in Q175DN mice. These data indicated that SUMO1 deletion altered the mHTT distribution in MSNs. Therefore, we further analyzed the distribution of EM48+ mHTT aggregates in the cell soma, nucleus, and extracellular space by confocal imaging.

Any EM48+ aggregates detected outside DAPI/DARPP-32 MSN were considered extracellular (see artistic rendering, Fig. 4K), following a guideline from a prior work (41). We detected nuclear aggregates using a nuclei marker (DAPI) and identified the cytoplasmic aggregates of EM48+ mHtt localized with DARPP-32, primarily a cytoplasmically localized protein in the MSN (see artistic rendering, Fig. 4K) (see Materials and Methods for details).

We found that the number of nuclear EM48+ aggregates (solid arrowhead, Fig. 4J and L) was significantly diminished in the DARPP-32+ neurons in the Q175DN-SUMO1KO mice compared with the Q175DN mice (Fig. 4J and L). Similarly, the extracellular EM48+ aggregates (asterisk) were significantly diminished in Q175DN-SUMO1KO mice compared with the Q175DN mice (Fig. 4J and M). In contrast, the cytoplasmic EM48+ aggregates (open arrowhead) in DARPP-32+ neurons were significantly increased in the Q175DN-SUMO1KO mice compared with the Q175DN mice (Fig. 4J and N). There was no significant difference in the number of cells (DAPI+) or total EM48+ aggregates between the groups (Fig. 4O and P). However, there was a significant decrease in the size of EM48+ mHtt aggregates in the Q175DN-SUMO1KO versus Q175DN mice (Fig. 4Q). The frequency distribution of various EM48+ puncta showed subtle variations across different sizes between Q175DN-SUMO1KO versus Q175DN mice (*SI Appendix, Fig. S6*). Thus, biochemical data and confocal microscopy findings indicate that SUMO1 deletion altered the mHtt aggregate dynamics and increased the steady-state levels of cytoplasmic EM48+ mHtt in the MSNs.

SUMO1 Deletion Regulates the p62 and EM48+ Interaction and Autophagic Activities in the Striatum. Next, we explored possible mechanisms for the regulation of Htt/mHtt levels by SUMO1 in the striatum. Prior works showed autophagy might regulate mHtt levels, so we focused on autophagy evaluation *in vivo* using organelle fractionation/western blotting and IHC assays. p62, a selective, well-established autophagy cargo, is incorporated within the autophagosomes (detected by LC3B-II) and degraded upon fusing with lysosomes. Moreover, previous studies have identified p62 as a critical mediator of HTT-induced selective autophagy and disease phenotype. So, we focused on subcellular localization of p62 and LC3B-II levels by western blotting and IHC in whole brain lysates and brain sections, respectively.

We separated lysosomes and mitochondria using sucrose density gradient centrifugation and found enhanced p62 and LC3B-II accumulation in the lysosomal fractions in the Q175DN-SUMO1KO (green oval) compared with the Q175DN striatum (red oval) (*SI Appendix, Fig. S7A*). The SUMO1KO mice also displayed enhanced p62 and LC3-II accumulation (blue rectangle) in the lysosomal fraction compared with the WT (black rectangle) (*SI Appendix, Fig. S7B*). This accumulation is unlikely due to diminished lysosomal activities because SUMO1 deletion provides strong protection against HD-related deficits (Figs. 1 and 2), and previous studies pointed out that lysosomal activities (Cathepsin D and Cathepsin B proteolytic enzymatic activities) are unaltered by mHTT (42). Moreover, mRNA levels of these enzymes were also unaltered in the striatum of Q175DN-SUMO1KO mice compared with Q175DN (*Dataset S1*). Thus, biochemical results indicated that SUMO1 regulates autophagic activities in the striatum *in vivo*. We also found that the mRNA levels of p62, Nbr1, Nrx1, and optn, the autophagy receptors associated with HD (43), showed a decreased trend in Q175DN-SUMO1KO striatum (*SI Appendix, Fig. S7C*).

Next, we carried out IHC to visualize EM48+ mHtt aggregates and its association with selected autophagic machineries. By applying fluorescence colocalization analysis using Mander's overlap coefficient (MOC), we found that p62 strongly associated with EM48+ aggregates in Q175DN striatum and that the

association was significantly diminished in the Q175DN-SUMO1KO striatum (arrowhead, Fig. 5A and B).

Simultaneous binding occurs between p62 and autophagosomes via the interaction with LC3B-II and between p62 and mHtt/Htt (44, 45). We used the MOC to examine the association of EM48+ mHtt and LAMP1 (a lysosomal marker), the association between LC3B-II and LAMP1, and the association between p62 and LAMP1. We found strong increases in the EM48 colocalization with LAMP1 (arrowhead, Fig. 5C and D) as well as enhanced interaction between LC3B and LAMP1 (arrowhead, Fig. 5E and F). By contrast, the p62 and LAMP1 association was diminished in the Q175DN-SUMO1KO striatum compared with the Q175DN striatum (arrowhead, Fig. 5G and H).

Collectively, our subcellular localization results indicate that SUMO1 deletion may enhance EM48+ mHtt association with lysosomes via autophagy activities in the HD striatum.

SUMO1 Deletion Increases Autophagy Activation and Diminishes mHtt in a Cellular Model of HD. We next used cultured HD striatal cells to examine the cause-and-effect relationship between SUMO1 and autophagy regulation. We depleted SUMO1 by CRISPR/Cas-9 in well-established *STHdh*^{Q7/Q7} (WT-control) and *STHdh*^{Q7/Q111} (HD-het) cell lines and successfully depleted ~50 to 60% of the SUMO1 modifications (Fig. 6A and B). The steady-state levels of Htt were not significantly affected by diminished SUMOylation in SUMO1-depleted (SUMO1Δ) WT-control and HD-het cells (Fig. 6A and B). The HD-het cells showed enhanced basal LC3B-II compared with WT-control, and the levels were not affected by SUMO1 depletion (Fig. 6A and B). By contrast, enhancement of p62 in HD-het cells was diminished by SUMO1 depletion (Fig. 6A and B).

As the degradation of p62 is an important indicator of autophagy status (autophagy flux), in addition to increased LC3B-II levels, we carried out subcellular fractionation to assess autophagy (46). We found LC3B-II (blue circle) and p62 (red circle) levels are accumulated in the lysosomal compartments in SUMO1Δ cells compared with ctrl WT-control cells (Fig. 6C and D). Interestingly, we found enhanced accumulation of LC3B-II (orange circle) but diminished p62 (green circle) in the lysosomal compartments of SUMO1Δ-HD-het cells compared with ctrl HD-het cells (Fig. 6C and D). This result suggests that SUMO1 deletion regulates autophagy activities in HD. Chloroquine experiments showed further accumulation of LC3B-II in SUMO1Δ-HD-het cells (Fig. 6E and F), indicating that SUMO1 most likely increases autophagy flux.

Next, we analyzed interaction of EM48+ mHtt aggregates with lysosomal machineries in SUMO1Δ HD-het cells. Results showed that colocalization of EM48-p62 (Fig. 6G and H), LAMP1-p62 (Fig. 6I and J), and EM48-LAMP-p62 (Fig. 6K and L) were decreased in SUMO1Δ HD-het cells compared with SUMO1 intact HD-het cells (ctrl). These results suggest that autophagy activities and mHtt interaction with lysosomal components are increased upon SUMO1 deletion in HD cells.

Unlike the *in vivo* paradigm (Fig. 4), we did not observe any drastic decline in basal Htt levels in SUMO1Δ HD-het cultured cells (Fig. 6A and B). One reason could be that the steady-state effect of SUMO1 on mHtt degradation by autophagy cannot be distinguishable from its synthesis. So, we carried out kinetic experiments with the protein synthesis inhibitor cycloheximide (CHX). The normal Htt levels were unaffected in SUMO1Δ WT-control in presence of CHX (*SI Appendix, Fig. S8A and B*), indicating that *in vivo* regulation of Htt by SUMO1 is perhaps regulated in a tissue- and age-dependent manner (Fig. 4). However, we found mHtt and polyQ mHtt levels were strongly diminished in the presence of CHX in the SUMO1Δ HD-het cells compared with the SUMO1 intact HD-het cells (ctrl) (*SI Appendix, Fig. S8A and B*). We also observed more autophagic activity evident by decreased p62

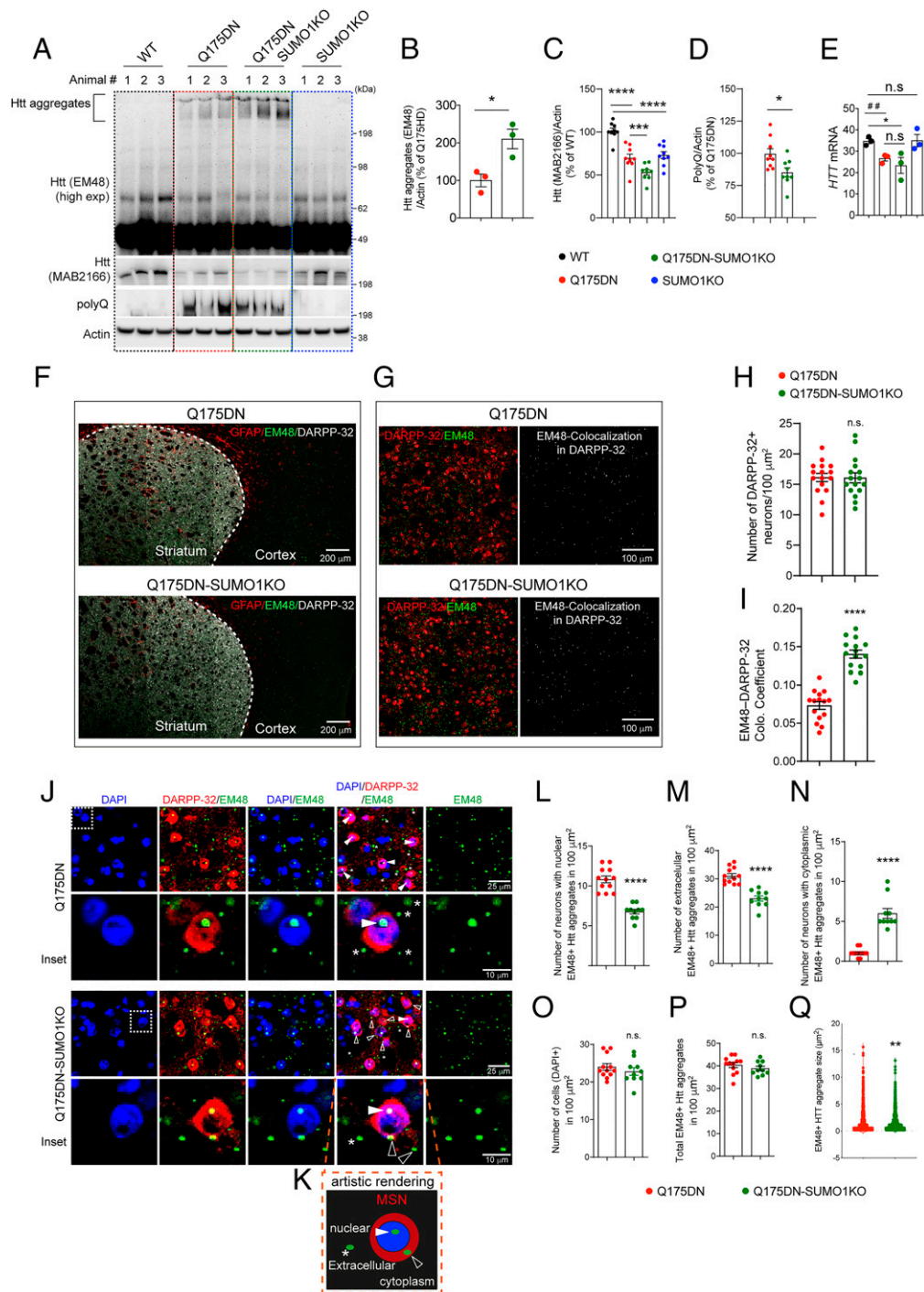


Fig. 4. SUMO1 deletion alters EM48 aggregate distribution in the Q175DN mice striatum. (A) Western blot for indicated proteins from the striatum tissues of indicated genotypes. (B–E) Quantification of the Htt aggregates (EM48) (B), Htt levels (MAB2166), and PolyQ (D) from A. Data are mean \pm SEM (B, $n = 3$, 2 male, 1 female; C and D, $n = 9$, 6 male, 3 female mice per genotype). * $P < 0.05$ by two-tailed unpaired Student's t test; *** $P < 0.001$, **** $P < 0.0001$ by one-way ANOVA followed by Tukey's multiple comparison test. (E) TPM (transcripts per kilobase million) counts of *Htt* mRNA from the RNA seq from striatum from indicated genotypes. Data are mean \pm SEM ($n = 3$, 2 male, 1 female, independent experiments). * $P < 0.05$ by one-way ANOVA followed by Tukey's multiple comparison test. ## $P < 0.01$ by two-tailed unpaired Student's t test. (F) Low-magnification confocal immunofluorescence images showing GFAP (red), Htt aggregates (EM48+, green), and DARPP-32 (white) expression from Q175DN and Q175DN-SUMO1KO brain sections. (G) Representative confocal images showing EM48+ Htt aggregates (green) and DARPP-32 (red) IHC and colocalization of EM48+ Htt aggregates and DARPP-32 in the striatum from Q175DN and Q175DN-SUMO1KO mice. (H) Bar graphs show the number of DARPP-32+ neurons in 100 μm^2 area. (I) MOC of EM48 and DARPP-32 from G. (J) Confocal images showing the EM48+ Htt aggregates (green), DARPP-32 (red) IHC, and DAPI. Lower panels show the magnified insets depicting nuclear EM48+ Htt aggregates (solid arrowhead), cytoplasmic EM48+ aggregates (open arrowhead) in the DARPP-32+ neuron, and extracellular EM48+ aggregates (asterisk). Artistic rendering of Htt aggregate distribution in and around MSN (K). (L–Q) Quantifications for the number of neurons with nuclear EM48+ aggregates (L), extracellular EM48+ Htt aggregates (M), cytoplasmic EM48+ Htt aggregates (N) in 100 μm^2 area, total number of cells (DAPI+) (O), total EM48+ Htt aggregates (P), and EM48+ Htt aggregate size (Q). (H, I, and L–Q) Data are mean \pm SEM ($n = 5$ mice per group [male = 3, female = 2]; three to four sections were analyzed for each striatal region per mouse). ** $P < 0.01$, **** $P < 0.0001$, unpaired two-tailed Student's t test. n.s., not significant.

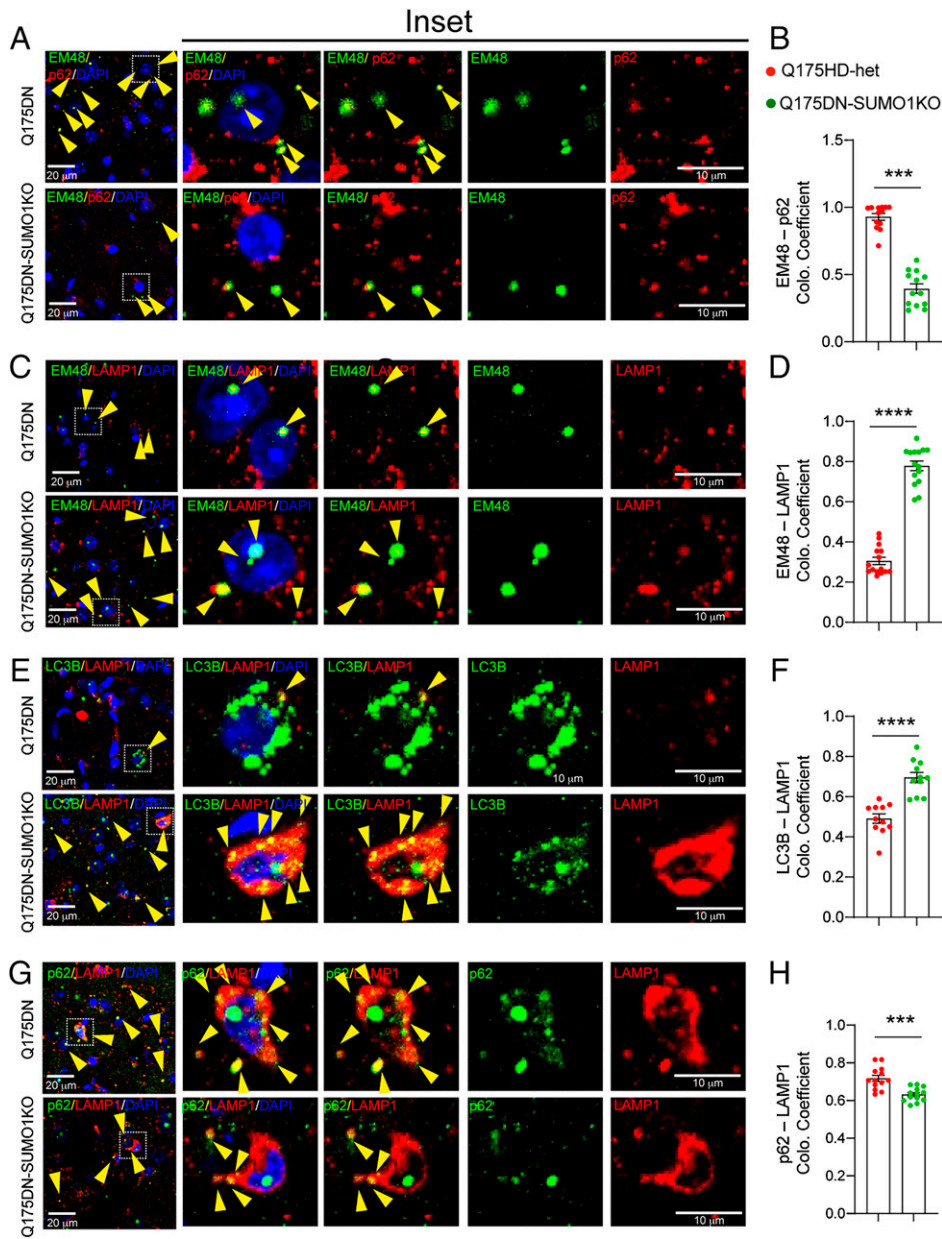


Fig. 5. SUMO1 deletion regulates autophagic activities in the striatum. (A–H) IHC and quantification for colocalization coefficients for EM48-p62 (A and B), EM48-LAMP1 (C and D), LC3B-LAMP1 (E and F), and p62-LAMP1 (G and H) in the striatum from Q175DN and Q175DN-SUMO1KO mice. DAPI (blue) and color channels (green or red) are shown according to the indicated antibody combination. Insets with magnified images are shown on the right. Yellow arrowheads indicate the colocalization for green and red channels. Data are mean \pm SEM ($n = 5$ mice per group [male = 3, female = 2]; from each mouse, four areas were averaged from two to four sections and section averages were used for analysis). *** $P < 0.001$, **** $P < 0.0001$ by two-tailed unpaired Student's t test.

and increased LC3B-II expression in the SUMO1 Δ HD-het cells (*SI Appendix, Fig. S8 A and B*). These results indicate SUMO1 deletion diminishes mHtt levels by enhancing autophagic activities in HD striatal cell model.

The SUMOylation Inhibitor Ginkgolic Acid Enhances Autophagy in Neuronal HD Cells and Human HD Fibroblasts. We then examined whether the pharmacological modulation of SUMOylation affected autophagy activities in HD cells. To determine this, we investigated the effect of ginkgolic acid (GA). GA, an extract from *Ginkgo biloba* leaves, is a type of alkyl phenol that can directly bind SUMO-activating enzyme, E1, and inhibit the formation of the E1-SUMO intermediate, thereby diminishing SUMOylation (47). Because SUMO1 depletion enhanced autophagic activities in HD, we hypothesized that GA might enhance the autophagy activities and alter HTT levels in HD cells. We tested the GA effect in WT-control, HD-het striatal neuronal cells, and human unaffected fibroblasts with 17 CAG repeats and HD-het fibroblasts that contain mHTT with 69 CAG repeats (this is closer to the form of mHTT in juvenile HD).

Treatment with various concentrations of GA (500 nM, 10 μ M, and 100 μ M) revealed 100 μ M induced strong autophagic activities in striatal neuron cells (*SI Appendix, Fig. S8 C and D*), consistent with prior work in neuroblastoma and epithelial cells (48, 49). Then, we found GA (100 μ M) resulted in two major effects in our cell models. First, at 0 h, GA induced a remarkable up-regulation of LC3B-II and p62 expression in striatal cells (Fig. 7A and B) as well as fibroblasts (Fig. 7C and D). Second, upon time-course experiments with CHX, the GA treatment did not affect normal HTT or mTOR levels either in WT striatal neuronal cells (Fig. 7A and B) or unaffected fibroblasts (Fig. 7C and D). However, GA showed a strong trend of diminished mHTT levels, particularly evident with polyQ antibodies in both cell types, and the diminishing effect of GA appeared more pronounced in the human HD fibroblast (Fig. 7B and D). Moreover, in CHX treatment, we observed time-dependent rapid degradation of the autophagic cargo p62 in HD striatal cells and human fibroblast cells in presence of GA compared with vehicle-treated controls (Fig. 7A–D). This data clearly indicates SUMOylation inhibitor GA promotes robust

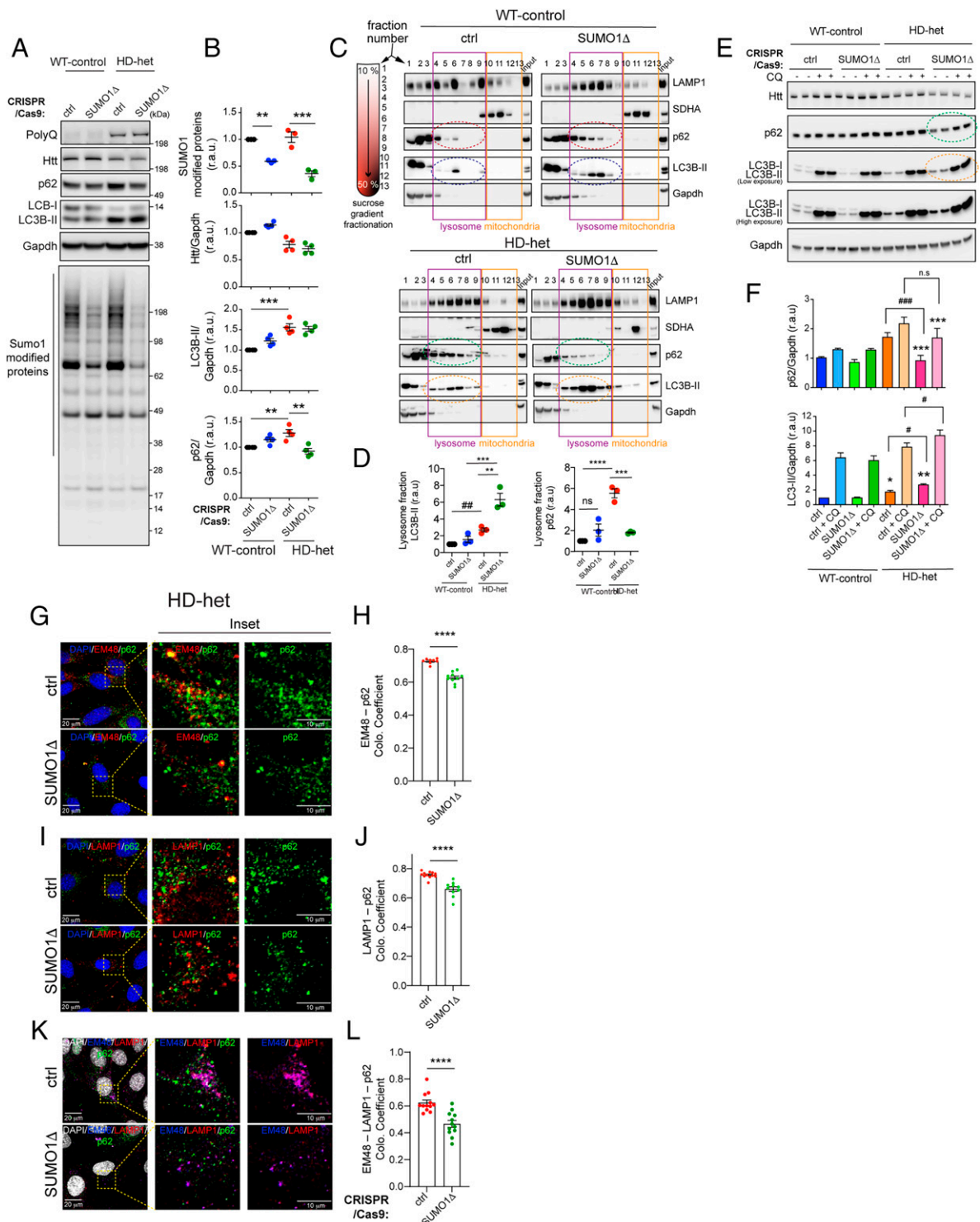


Fig. 6. SUMO1 deletion increases the autophagy in a cellular model of HD. (A) Western blotting of the indicated proteins in control (ctrl) and SUMO1-depleted (SUMO Δ) WT-control and HD-het striatal cells. (B) Quantification of the indicated proteins from A. Data are mean \pm SEM ($n = 3$ to 4 independent experiments). ** $P < 0.01$, *** $P < 0.001$ by one-way ANOVA followed by Tukey's multiple comparison test. (C) Western blot of subcellular fractionation from ctrl and SUMO Δ WT-control and HD-het striatal cells. Purple and orange rectangles show lysosomal and mitochondrial fractions, respectively. Dotted ovals show enrichment of the indicated proteins. (D) Western blot quantification of lysosomal LC3B-II and p62 for the control and SUMO Δ WT and HD-het cells. Data are mean \pm SEM; $n = 3$ independent experiments; ** $P < 0.01$, *** $P < 0.001$, and **** $P < 0.0001$ by two-way ANOVA followed by Tukey's multiple comparison test or ## $P < 0.01$ by two-tailed unpaired Student's t test. (E and F) Western blotting of the indicated proteins in ctrl and SUMO Δ WT-control and HD-het striatal cells without or with chloroquine (CQ) 50 μ M treatment (E) and the corresponding quantifications (F) * $P < 0.05$, ** $P < 0.01$, and *** $P < 0.001$ versus WT-control, by two-way ANOVA followed by Tukey's multiple comparison test or # $P < 0.05$, ## $P < 0.001$ by two-tailed unpaired Student's t test. (G–L) Confocal images and corresponding magnified insets of ctrl and SUMO Δ -HD-het cells immunostained and showing quantification of Mander's colocalization coefficient for EM 48-p62 (G and H), LAMP1-p62 (I and J), and EM48-LAMP1-p62 (K and L). Data are mean \pm SEM ($n = 4$ independent experiments; from each experiment, two to three 100- μ m² areas were quantified and used for group analysis). **** $P < 0.0001$ by two-tailed unpaired Student's t test.

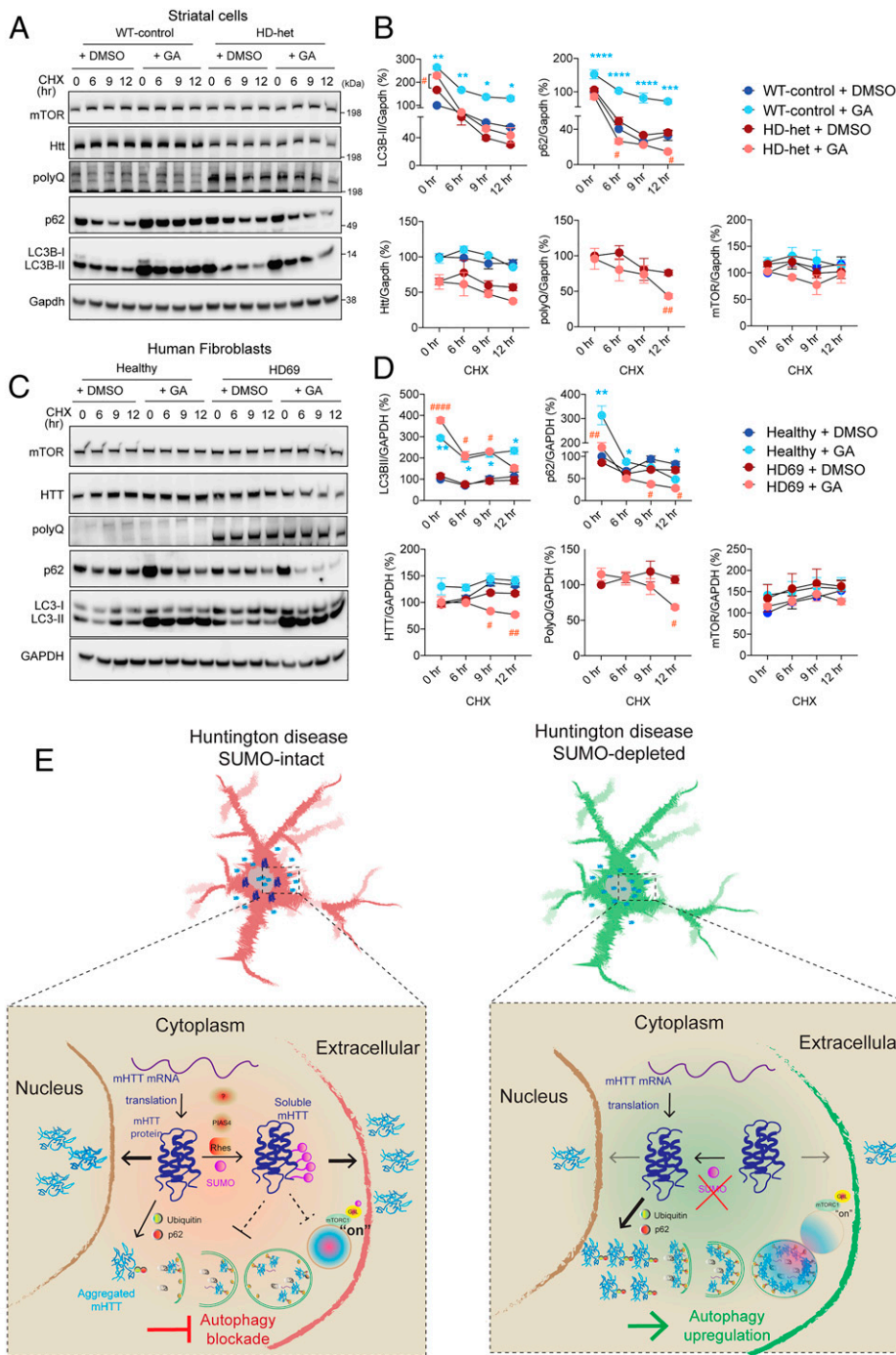


Fig. 7. SUMO inhibition by GA decreases steady-state levels of mHTT in HD striatal and human HD fibroblasts. (A) Representative western blot for the indicated proteins from WT-control and HD-het cells treated with vehicle dimethylsulfoxide (DMSO) or GA (100 μ M) for 24 h and CHX (75 μ M) for the indicated time points. (B) Quantification of indicated proteins from A. Data are mean \pm SEM ($n = 3$ independent experiments); * $P < 0.05$, ** $P < 0.01$, *** $P < 0.001$, and **** $P < 0.0001$ between WT-control and WT-control + GA; * $P < 0.05$, and ## $P < 0.01$ between HD-het and HD-het + GA by repeated measure two-way ANOVA followed by Tukey's multiple comparison test or Bonferroni's multiple comparisons test (for PolyQ). (C) Human fibroblast healthy or patient-derived HD cells (HD 69) treated with GA (100 μ M) for 24 h and CHX (50 μ M) for the indicated time points. (D) Quantification of indicated proteins from C. Data are mean \pm SEM ($n = 3$ independent experiments); * $P < 0.05$, and ** $P < 0.01$ between healthy and healthy + GA; # $P < 0.05$, ## $P < 0.01$, and ### $P < 0.0001$ between HD69 and HD69 + GA by repeated measure two-way ANOVA followed by Tukey's multiple comparison test or Bonferroni's multiple comparisons test (for PolyQ). (E) A mechanistic model depicting SUMO1-mediated striatal abnormalities in HD. See Discussion for details.

autophagy and rapid clearance of autophagy cargo. The effect of GA is specific to mHTT because GA did not influence normal HTT or mTOR levels compared with vehicle controls (Fig. 7 A–D). These results indicate that GA mimics SUMO1 depletion and potentiates autophagy activities and diminishes mHTT protein levels in both mouse and human HD cells.

Discussion

Although polyglutamine expansion is sufficient for pathogenesis, the toxicity of mHTT is altered by additional cis/trans regulators. Previous studies have revealed that SUMO is a transacting regulator of mHTT toxicity in HD cells and in HD animal models.

SUMO modification of mHTT increases the soluble forms to promote cellular toxicity (21–23, 50), but no in vivo role or underlying mechanism for SUMOylation has been proposed for HD pathogenesis in the knockin model.

The present data reveal that SUMO1 deletion in the Q175DN HD-het knockin mice diminished HD-related behavioral and anatomical deficits and inflammatory responses and was accompanied by the enhancement of EM48⁺/p62 localization, autophagy, and lysosomal activities in the striatum. Interestingly, the SUMO1-deleted MSNs showed alteration of mHTT from a soluble to an aggregated state, and the aggregates were then further reallocated from the nucleus and extracellular space to the cytoplasm. Thus, in the presence of SUMO1 the HD

pathogenesis is accompanied by aberrant autophagy signaling and a potentially neurotoxic localization of soluble forms of mHTT in the cytoplasm.

Interestingly, we found SUMO2/3 mRNAs are significantly enhanced in Q175DN mice striatum but appear to be decreased in Q175DN-SUMO1KO. Moreover, the autophagy regulator gene (Atg 5, but not other Atgs (3, 8, 10, or 13), is significantly up-regulated in Q175DN-SUMO1KO. Pink1, a positive regulator of autophagy, is diminished in Q175DN-SUMO1KO (*SI Appendix, Fig. S9 A and B*). These results reveal that the possible mechanism(s) may involve specific transcriptional/posttranscriptional regulation of SUMO isoform signaling and a specific autophagy regulatory mechanism in the mediation of mHTT-induced striatal atrophy.

Previous studies have linked SUMOylation to autophagy. For example, SUMOylation of Vps34 and its interaction with Beclin-1 is implicated in autophagosome formation in cancer and smooth muscle cells (51, 52). Similarly, the SUMO E2 ligase Ubc9 can regulate autophagy flux in cardiomyocytes (53). Upon DNA damage, SUMOylation of RhoB promotes its interaction with TSC2 and translocation to the lysosomes, where it inhibits mTORC1 to result in activation of autophagy (54). Furthermore, deletion of the *Semp3* gene that codes for a de-SUMOylating enzyme increased autophagy flux in the liver (55). These results suggest that SUMOylation promotes autophagy flux. By contrast, blocking the SUMO pathway by depleting SUMO1 and UBC9 or by exposure to ginkgolic acid (a SUMOylation inhibitor) enhances the autophagy flux in breast cancer cells (56). Thus, SUMOylation can modulate autophagy in two opposite directions depending on the cell/tissue type, regulator, and targets of the SUMO pathway being altered. Therefore, a highly complex and intricate regulation of SUMOylation is associated with autophagy dysregulation, which may interfere with various kinds of autophagy including macroautophagy and chaperone-mediated autophagy (57).

The autophagy dysregulation mechanisms in HD may involve a combination of multiple molecular processes. For example, SUMO1 modification of mHTT may directly interfere with the autophagy components; consequently, a loss of SUMO1 increases the levels of the ubiquitinated version of mHTT that, in turn, can interact strongly with p62 to enhance macroautophagy as well as mHTT clearance (*Fig. 7E*). This possibility is supported by our results showing enhanced autophagy activities and degradation of soluble mHTT in SUMO1-deleted HD striatum and cell models. SUMO may also inhibit autophagy via an indirect and integrated inhibitor feedback loop. For instance, 1) SUMO modification of GβL (58), which is a major component of mTOR, regulates nutrient-induced mTORC1 signaling, which inhibits autophagy; 2) SUMO modification of mHTT, which also promotes nutrient-induced mTORC1 signaling (32), may further inhibit autophagy; and 3) SUMOylation of Rhes on multiple sites may regulate Rhes-mediated Beclin-1-dependent and mTOR-independent autophagy (20, 59). Thus, SUMO deletion may regulate autophagy in the striatum via both mTOR-dependent and mTOR-independent signaling pathways, but the precise mechanisms of actions are unclear.

Despite enhanced astroglial and microglial response in HD striatum, only a limited number of gene transcripts and the associated inflammatory biomarkers were altered in the striatum of SUMO1-deleted HD mice (*Dataset S1*). The exact details of how autophagy and inflammation are linked in the regulation of CNS functions and disease remains unclear, but autophagy is known to play a critical role in neuroinflammation by a repertoire of the process including the survival of inflammatory cells—for example, astrocytes and microglia (60). In fact, autophagy inhibition is shown to promote astrocytic malfunction (61). Moreover, we showed that cyclic GMP-AMP synthase (cGAS), a DNA sensor, is up-regulated in HD and promotes

autophagy and inflammatory responses in the HD cell model (62). How cGAS and SUMO may interact in HD remains unknown. Thus, SUMO1–autophagy dysregulation may synergize with upstream inflammatory regulators to promote HD-like deficits.

We propose a model (*Fig. 7E*) whereby mHTT is synthesized and then undergoes SUMO modification, mediated by one or more SUMO E3-like proteins, such as Rhes (19, 20, 23), PIAS (21, 50), or unknown E3s. Both the non-SUMOylated and SUMOylated versions of mHTT can move from cytoplasm into the nucleus and out of the neurons (into the extracellular space) and eventually become aggregated. A portion of the non-SUMOylated HTT that aggregates in the cytoplasm is removed by the ubiquitin and p62 interaction through autophagy or other degradation pathways such as proteasomes (63). By contrast, the SUMOylated soluble mHTT forms in cytoplasm inhibit autophagy either by activating mTORC1 or blocking autophagosome formation or lysosomal activities. Thus, SUMO1 causes a slow and sustained blockade of autophagy, thereby affecting neuronal homeostasis and leading to the MSN dysfunction observed in HD (*Fig. 7E, Left*). Lack of SUMO1 averts this autophagy inhibition and impedes the transport of mHTT to the nucleus and extracellular space. This enhances the formation of mHTT aggregates in the cytoplasm, and these can now be degraded through the active autophagy pathway (*Fig. 7E, Right*).

Surprisingly, the SUMO E3-like protein Rhes levels are down-regulated in the Hdh150Q knockin mouse striatum (64), indicating that compensatory mechanisms are at work. Perhaps clearance of Rhes will decrease the SUMOylated forms of mHTT and extend the onset and reduce the severity of the disease process. Consistent with this notion, forced expression of Rhes enhanced soluble forms of mHTT and worsened the motor phenotype in HD mouse models (65). We could not quantify the SUMOylation of endogenous FL-HTT due to low stoichiometry of SUMOylation of FL-HTT in vivo. Interestingly, we found that Rhes can disseminate mHTT in the brain (66), but whether this requires SUMO remains to be determined.

Overall, this report, based on data integrated from in vivo and in vitro models, behavioral approaches, and biochemical tools, provides insights into a critical role of SUMO in autophagy regulation in HD. SUMO1 deletion reduces the soluble mHTT levels, prevents the inflammatory response, and ameliorates HD pathogenesis. This research shows that interfering with SUMO signaling, for example, by using a pharmacological inhibitor such as GA or its analogs, can provide therapeutic opportunities to relieve HD symptoms and progression by up-regulating autophagy and diminishing toxic mHTT levels.

Materials and Methods

Reagents, antibodies, animals and behavioral assay, cell lines, biochemical analysis, immunohistochemistry, mHTT aggregation assay, lateral ventricle area determination, stereology, immunocytochemistry, RNA Seq, and statistical analysis can be found in *SI Appendix, Materials and Methods*.

Data Availability. All study data are included in the article and/or *SI Appendix*. Sequencing data have been submitted to the Gene Expression Omnibus data repository (*GSE150990*). All other study data are included in the article and/or supporting information.

ACKNOWLEDGMENTS. We thank Melissa Benilous and members at the Scripps Proteomics and Genomics Core for their help and expertise. We thank Dr. Baoji and his laboratory member, Heng Li, for Iba1 antibody. This research was partially supported by a training grant in Alzheimer's drug discovery from the Lottie French Lewis Fund of the Community Foundation for Palm Beach and Martin Counties, grant awards from NIH/National Institute for Neurological Disorders and Stroke (NINDS), Nos. R01-NS087019-01A1 and R01-NS094577-01A1, a grant from the Cure for Huntington Disease Research Initiative Foundation, and Scripps bridge funding.

1. P. McColgan *et al.*, Track-HD Investigators, Selective vulnerability of Rich Club brain regions is an organizational principle of structural connectivity loss in Huntington's disease. *Brain* **138**, 3327–3344 (2015).
2. S. J. Tabrizi, M. D. Flower, C. A. Ross, E. J. Wild, Huntington disease: New insights into molecular pathogenesis and therapeutic opportunities. *Nat. Rev. Neurol.* **16**, 529–546 (2020).
3. G. Schilling *et al.*, Expression of the Huntington's disease (IT15) protein product in HD patients. *Hum. Mol. Genet.* **4**, 1365–1371 (1995).
4. F. R. Fusco *et al.*, Cellular localization of huntingtin in striatal and cortical neurons in rats: Lack of correlation with neuronal vulnerability in Huntington's disease. *J. Neurosci.* **19**, 1189–1202 (1999).
5. G. B. Landwehrmeyer *et al.*, Huntington's disease gene: Regional and cellular expression in brain of normal and affected individuals. *Ann. Neurol.* **37**, 218–230 (1995).
6. S. Finkbeiner, The autophagy lysosomal pathway and neurodegeneration. *Cold Spring Harb. Perspect. Biol.* **12**, a033993 (2020).
7. M. Shibata *et al.*, Regulation of intracellular accumulation of mutant huntingtin by Beclin 1. *J. Biol. Chem.* **281**, 14474–14485 (2006).
8. L. M. Fox *et al.*, Huntington's disease pathogenesis is modified in vivo by Alfy/Wdfy3 and selective macroautophagy. *Neuron* **105**, 813–821.e6 (2020).
9. M. Martinez-Vicente *et al.*, Cargo recognition failure is responsible for inefficient autophagy in Huntington's disease. *Nat. Neurosci.* **13**, 567–576 (2010).
10. Y. N. Rui, Z. Xu, B. Patel, A. M. Cuervo, S. Zhang, HTT/Huntingtin in selective autophagy and Huntington disease: A foe or a friend within? *Autophagy* **11**, 858–860 (2015).
11. J. Ochaba *et al.*, Potential function for the huntingtin protein as a scaffold for selective autophagy. *Proc. Natl. Acad. Sci. U.S.A.* **111**, 16889–16894 (2014).
12. K. R. Croce, A. Yamamoto, A role for autophagy in Huntington's disease. *Neurobiol. Dis.* **122**, 16–22 (2019).
13. M. Martinez-Vicente, Novel therapeutic approach to induce autophagy in a *Drosophila* model for Huntington's disease. *Cells* **9**, E495 (2020).
14. S. Sarkar, B. Ravikumar, R. A. Floto, D. C. Rubinsztein, Rapamycin and mTOR-independent autophagy inducers ameliorate toxicity of polyglutamine-expanded huntingtin and related proteinopathies. *Cell Death Differ.* **16**, 46–56 (2009).
15. R. Aron *et al.*, Deubiquitinase Usp12 functions noncatalytically to induce autophagy and confer neuroprotection in models of Huntington's disease. *Nat. Commun.* **9**, 3191 (2018).
16. J. F. Moruno Manchon *et al.*, Cytoplasmic sphingosine-1-phosphate pathway modulates neuronal autophagy. *Sci. Rep.* **5**, 15213 (2015).
17. K. S. Abd-Elrahman *et al.*, mGluR5 antagonism increases autophagy and prevents disease progression in the zQ175 mouse model of Huntington's disease. *Sci. Signal.* **10**, eaan6387 (2017).
18. Z. Li *et al.*, Allele-selective lowering of mutant HTT protein by HTT-LC3 linker compounds. *Nature* **575**, 203–209 (2019).
19. S. Subramaniam *et al.*, Rhes, a physiologic regulator of sumoylation, enhances cross-sumoylation between the basic sumoylation enzymes E1 and Ubc9. *J. Biol. Chem.* **285**, 20428–20432 (2010).
20. O. Rivera *et al.*, Rhes, a striatal enriched protein, regulates post-translational small-ubiquitin-like-modifier (SUMO) modification of nuclear proteins and alters gene expression. *bioRxiv* [Preprint] 10.1101/2020.06.18.160044 (2020).
21. J. G. O'Rourke *et al.*, SUMO-2 and PIAS1 modulate insoluble mutant huntingtin protein accumulation. *Cell Rep.* **4**, 362–375 (2013).
22. J. S. Steffan *et al.*, SUMO modification of huntingtin and Huntington's disease pathology. *Science* **304**, 100–104 (2004).
23. S. Subramaniam, K. M. Sixt, R. Barrow, S. H. Snyder, Rhes, a striatal specific protein, mediates mutant-huntingtin cytotoxicity. *Science* **324**, 1327–1330 (2009).
24. M. Sharma, S. Subramaniam, Rhes travels from cell to cell and transports Huntington disease protein via TNT-like protrusion. *J. Cell Biol.* **218**, 1972–1993 (2019).
25. S. Subramaniam, Selective neuronal death in neurodegenerative diseases: The ongoing mystery. *Yale J. Biol. Med.* **92**, 695–705 (2019).
26. Q. Liu *et al.*, Loss of Hap1 selectively promotes striatal degeneration in Huntington disease mice. *Proc. Natl. Acad. Sci. U.S.A.* **117**, 20265–20273 (2020).
27. I. Hernandez *et al.*, A farnesyltransferase inhibitor activates lysosomes and reduces tau pathology in mice with tauopathy. *Sci. Transl. Med.* **11**, eaat3005 (2019).
28. A. J. Ehrenberg *et al.*, Patterns of neuronal Rhes as a novel hallmark of tauopathies. *Acta Neuropathol* **141**, 651–666 (2021).
29. A. L. Southwell *et al.*, An enhanced Q175 knock-in mouse model of Huntington disease with higher mutant huntingtin levels and accelerated disease phenotypes. *Hum. Mol. Genet.* **25**, 3654–3675 (2016).
30. G. A. Smith *et al.*, Progressive axonal transport and synaptic protein changes correlate with behavioral and neuropathological abnormalities in the heterozygous Q175 KI mouse model of Huntington's disease. *Hum. Mol. Genet.* **23**, 4510–4527 (2014).
31. L. B. Menalled *et al.*, Comprehensive behavioral and molecular characterization of a new knock-in mouse model of Huntington's disease: zQ175. *PLoS One* **7**, e49838 (2012).
32. W. M. Pryor *et al.*, Huntingtin promotes mTORC1 signaling in the pathogenesis of Huntington's disease. *Sci. Signal.* **7**, ra103 (2014).
33. T. Heikkinen *et al.*, Characterization of neurophysiological and behavioral changes, MRI brain volumetry and 1H MRS in zQ175 knock-in mouse model of Huntington's disease. *PLoS One* **7**, e50717 (2012).
34. P. Langfelder *et al.*, Integrated genomics and proteomics define huntingtin CAG length-dependent networks in mice. *Nat. Neurosci.* **19**, 623–633 (2016).
35. M. Terao *et al.*, Mouse aldehyde-oxidase-4 controls diurnal rhythms, fat deposition and locomotor activity. *Sci. Rep.* **6**, 30343 (2016).
36. D. B. Bloch *et al.*, Sp110 localizes to the PML-Sp100 nuclear body and may function as a nuclear hormone receptor transcriptional coactivator. *Mol. Cell. Biol.* **20**, 6138–6146 (2000).
37. T. Muinao, M. Pal, H. P. D. Boruah, Cytosolic and transmembrane protein extraction methods of breast and ovarian cancer cells: A comparative study. *J. Biomol. Tech.* **29**, 71–78 (2018).
38. S. J. Cordwell, Sequential extraction of proteins by chemical reagents. *Methods Mol. Biol.* **424**, 139–146 (2008).
39. W. Reindl *et al.*, Meso scale discovery-based assays for the detection of aggregated huntingtin. *PLoS One* **14**, e0213521 (2019).
40. V. Fodale *et al.*, Analysis of mutant and total huntingtin expression in Huntington's disease murine models. *Sci. Rep.* **10**, 22137 (2020).
41. N. Carty *et al.*, Characterization of HTT inclusion size, location, and timing in the zQ175 mouse model of Huntington's disease: An in vivo high-content imaging study. *PLoS One* **10**, e0123527 (2015).
42. Q. Liang, X. Ouyang, L. Schneider, J. Zhang, Reduction of mutant huntingtin accumulation and toxicity by lysosomal cathepsins D and B in neurons. *Mol. Neurodegener.* **6**, 37 (2011).
43. Z. Deng *et al.*, Autophagy receptors and neurodegenerative diseases. *Trends Cell Biol.* **27**, 491–504 (2017).
44. F. M. Menzies *et al.*, Autophagy and neurodegeneration: Pathogenic mechanisms and therapeutic opportunities. *Neuron* **93**, 1015–1034 (2017).
45. D. D. Martin, S. Ladha, D. E. Ehrnhoefer, M. R. Hayden, Autophagy in Huntington disease and huntingtin in autophagy. *Trends Neurosci.* **38**, 26–35 (2015).
46. D. J. Klionsky *et al.*, Guidelines for the use and interpretation of assays for monitoring autophagy (4th edition). *Autophagy* **17**, 1–382 (2021).
47. I. Fukuda *et al.*, Ginkgolic acid inhibits protein SUMOylation by blocking formation of the E1-SUMO intermediate. *Chem. Biol.* **16**, 133–140 (2009).
48. B. Chhunchha, P. Singh, D. P. Singh, E. Kubo, Ginkgolic acid rescues lens epithelial cells from injury caused by redox regulated-aberrant sumoylation signaling by reviving Prdx6 and Sp1 expression and activities. *Int. J. Mol. Sci.* **19**, E3520 (2018).
49. S. Vijayakumaran, Y. Nakamura, J. M. Henley, D. L. Pountney, Ginkgolic acid promotes autophagy-dependent clearance of intracellular alpha-synuclein aggregates. *Mol. Cell. Neurosci.* **101**, 103416 (2019).
50. J. Ochaba *et al.*, PIAS1 regulates mutant huntingtin accumulation and Huntington's disease-associated phenotypes in vivo. *Neuron* **90**, 507–520 (2016).
51. Y. Yang *et al.*, Acetylated hsp70 and KAP1-mediated Vps34 SUMOylation is required for autophagosome creation in autophagy. *Proc. Natl. Acad. Sci. U.S.A.* **110**, 6841–6846 (2013).
52. Y. Yao *et al.*, SUMOylation of Vps34 by SUMO1 promotes phenotypic switching of vascular smooth muscle cells by activating autophagy in pulmonary arterial hypertension. *Pulm. Pharmacol. Ther.* **55**, 38–49 (2019).
53. M. K. Gupta *et al.*, UBC9-mediated sumoylation favorably impacts cardiac function in compromised hearts. *Circ. Res.* **118**, 1894–1905 (2016).
54. M. Liu *et al.*, ATR/Chk1 signaling induces autophagy through sumoylated RhoB-mediated lysosomal translocation of TSC2 after DNA damage. *Nat. Commun.* **9**, 4139 (2018).
55. K. Liu *et al.*, A fine-tuning mechanism underlying self-control for autophagy: deSUMOylation of BECN1 by SENP3. *Autophagy* **16**, 975–990 (2020).
56. M. Lorente *et al.*, Inhibiting SUMO1-mediated SUMOylation induces autophagy-mediated cancer cell death and reduces tumour cell invasion via RAC1. *J. Cell Sci.* **132**, jcs234120 (2019).
57. A. M. Cuervo, S. Zhang, Selective autophagy and huntingtin: Learning from disease. *Cell Cycle* **14**, 1617–1618 (2015).
58. S. Park *et al.*, SUMO Modifies GβL and Mediates mTOR Signaling. 10.1101/2020.09.03.281881, *BioRxiv* (2020).
59. R. G. Mealer, A. J. Murray, N. Shahani, S. Subramaniam, S. H. Snyder, Rhes, a striatal-selective protein implicated in Huntington disease, binds beclin-1 and activates autophagy. *J. Biol. Chem.* **289**, 3547–3554 (2014).
60. E. Motori *et al.*, Inflammation-induced alteration of astrocyte mitochondrial dynamics requires autophagy for mitochondrial network maintenance. *Cell Metab.* **18**, 844–859 (2013).
61. A. Pla, M. Pascual, C. Guerri, Autophagy constitutes a protective mechanism against ethanol toxicity in mouse astrocytes and neurons. *PLoS One* **11**, e0153097 (2016).
62. M. Sharma, S. Rajendrarao, N. Shahani, U. N. Ramirez-Jarquín, S. Subramaniam, Cyclic GMP-AMP synthase promotes the inflammatory and autophagy responses in Huntington disease. *Proc. Natl. Acad. Sci. U.S.A.* **117**, 15989–15999 (2020).
63. T. Zhao, Y. Hong, S. Li, X. J. Li, Compartment-dependent degradation of mutant huntingtin accounts for its preferential accumulation in neuronal processes. *J. Neurosci.* **36**, 8317–8328 (2016).
64. J. Hernandez, N. Shahani, S. Swarnkar, S. Subramaniam, Rhes deletion prevents age-dependent selective motor deficits and reduces phosphorylation of S6K in Huntington Disease Hdh150Q(CAG) knock-in mice. *bioRxiv* [Preprint] 10.1101/2021.06.16.448681 (2021).
65. S. Swarnkar *et al.*, Ectopic expression of the striatal-enriched GTPase Rhes elicits cerebellar degeneration and an ataxia phenotype in Huntington's disease. *Neurobiol. Dis.* **82**, 66–77 (2015).
66. U. N. Ramirez Jarquin *et al.*, Rhes protein transits from neuron to neuron and facilitates mutant huntingtin spreading in the brain. *bioRxiv* [Preprint] 10.1101/2021.08.27.457956 (2021).